Journal of Orthopaedic Translation 26 (2021) 151–161

Contents lists available at ScienceDirect

Journal of Orthopaedic Translation

journal homepage: www.journals.elsevier.com/journal-of-orthopaedic-translation

Original article

A novel tissue-engineered bone graft composed of silicon-substituted calcium phosphate, autogenous fine particulate bone powder and BMSCs promotes posterolateral spinal fusion in rabbits

LiHuang Cui [1,2], ShouYang Xiang [1,2], DeChun Chen [1], Rui Fu [1], Xin Zhang [1], JingTao Chen [1], XinTao Wang [*,1]

Department of Orthopedic Surgery, The Second Affiliated Hospital of Harbin Medical University, Harbin, China

ARTICLE INFO

Keywords:
Autogenous fine particulate bone powder
Bone marrow mesenchymal stem cells
Bone tissue engineering
Silicate-substituted calcium phosphate
Spinal fusion

SUMMARY

Background: Autogenous bone graft is the gold standard bone grafting substrate available in spinal fusion because of its osteoconductive, osteogenic, and osteoinductive properties. However, several shortcomings including bleeding, infection, chronic pain, and nerve injury are known to be associated with the procedure. Bone tissue engineering has emerged as an alternative therapeutic strategy for bone grafts. New materials have been developed and tested that can substitute for the autogenous bone grafts used in the spinal fusion. The purpose of this study is to evaluate the role of a novel tissue-engineered bone graft with silicon-substituted calcium phosphate (Si-CaP), autogenous fine particulate bone powder (AFPBP), and bone marrow mesenchymal stem cells (BMSCs) using a rabbit posterolateral lumbar fusion model based on bone tissue engineering principles. The application of this graft can represent a novel choice for autogenous bone to reduce the amount of autogenous bone and promote spinal fusion.

Methods: BMSCs from New Zealand white rabbits were isolated and cultured in vitro. Then, BMSCs were marked by the cell tracker chloromethyl-benzamidodialkylcarbocyanine (CM-Dil). A total of 96 New Zealand White rabbits were randomly divided into four groups: (a) AFPBP, (b) Si-CaP, (c) Si-CaP/AFPBP, (d) Si-CaP/AFPBP/BMSCs.The rabbits underwent bilateral posterolateral spine arthrodesis of the L5-L6 intertransverse processes using different grafts. Spinal fusion and bone formation were evaluated at 4, 8, and 12 weeks after surgery by manual palpation, radiology, micro-computed tomography (micro-CT), histology, and scanning electronic microscopy (SEM).

Results: The rate of fusion by manual palpation was higher in the Si-CaP/AFPBP/BMSCs group than the other groups at 8 weeks. The fusion rates in the Si-CaP/AFPBP/BMSCs and the AFPBP groups both reached 100%, which was higher than the Si-CaP/AFPBP group (62.5%) ($P > 0.05$) and Si-CaP group (37.5%) ($P < 0.05$) at 12 weeks. New bone formation was observed in all groups after implantation by radiology and micro-CT. The radiographic and CT scores increased in all groups from 4 to 12 weeks, indicating a time-dependent osteogenetic process. The Si-CaP/AFPBP/BMSCs group showed a larger amount of newly formed bone than the Si-CaP/AFPBP and Si-CaP groups at 12 weeks. Bone formation in the Si-CaP/AFPBP/BMSCs group was similar to the AFPBP group. Histology showed that new bone formation continued and increased along with the degradation and absorption of Si-CaP and AFPBP from 4 to 12 weeks in the Si-CaP, Si-CaP/AFPBP, and Si-CaP/AFPBP/BMSCs groups. At 4 weeks, a higher proportion of bone was detected in the AFPBP group (23.49%) compared with the Si-CaP/AFPBP/BMSCs group (14.66%, $P < 0.05$). In the Si-CaP/AFPBP/BMSCs group at 8 weeks, the area percentage of new bone formation was 28.56%, which was less than the AFPBP group (33.21%, $P < 0.05$). No difference in bone volume was observed between the Si-CaP/AFPBP/BMSCs group (44.39%) and AFPBP group (45.06%) at 12 weeks ($P > 0.05$). At 12 weeks, new trabecular were visible in the Si-CaP/AFPBP/BMSCs group by

* Corresponding author.
E-mail address: xintaog6@163.com (X. Wang).
[1] Present Address: Department of Orthopedic Surgery, The Second Affiliated Hospital of Harbin Medical University, Xuefu Road 246, Harbin, Heilongjiang 150081, PR China.
[2] LiHuang Cui and ShouYang Xiang are co-first authors. These authors contributed equally to this work.

https://doi.org/10.1016/j.jot.2020.06.003
Received 5 March 2020; Received in revised form 10 June 2020; Accepted 15 June 2020
Available online 14 September 2020

SEM. CM-Dil-positive cells were observed at all stages. Compared with histological images, BMSCs participate in various stages of osteogenesis by transforming into osteoblasts, chondrocytes, and osteocytes.
Conclusion: This study demonstrated for the first time that Si-CaP/AFPBP/BMSCs is a novel tissue-engineered bone graft with excellent bioactivity, biocompatibility, and biodegradability. The graft could reduce the amount of autogenous bone and promote spinal fusion in a rabbit posterolateral lumbar fusion model, representing a novel alternative to autogenous bone.
The Translational potential of this article: The translational potential of this article lies in that this graft will be a novel spinal fusion graft with great potential for clinical applications.

Introduction

In the treatment of spinal degenerative diseases and other spinal diseases such as trauma, infection, tumor, and malformation, spinal fusion surgery is frequently required to restore spinal stability [1]. Autogenous bone grafts with osteoconductive, osteoinductive, and osteogenic properties are still considered the gold standard as an effective material for posterolateral fusion of the spine [2]. More than 1.5 million autogenous bone grafts are required annually for surgical procedures in the USA [3]. However, autogenous bone grafting has major disadvantages in several clinical situations, including an insufficient amount of graft material available for use, particularly for the treatment of large bone defects, and significant postoperative morbidity at the donor site in 8% of patients, such as bleeding, infection, chronic pain, deformity, scarring, nerve injury, increased operative time, and additional cost [4,5].

Thus, finding a suitable strategy to replace the autogenous bone graft is an important task for improved clinical outcomes. One strategy is to construct a tissue-engineered bone graft with bone particles and certain scaffold materials to replace the autogenous bone graft [6]. Bone tissue engineering aims to avoid problems associated with bone grafting by using degradable scaffolds enriched with stem cells and/or growth factors [7].

Scaffolds can be called “the beating heart” of the tissue engineering field. Without the appropriate scaffold, the growth of cells in an artificial environment is not possible. Biodegradable scaffold materials can be taxonomized into ceramics, polymers, metals, and composites [8]. Silicon-substituted calcium phosphate (Si-CaP) constitutes a newer generation of ceramics produced by the addition of calcium and silicate to its phosphate core. In previous studies, Si-CaP appeared to provide a more stable osteoconductive scaffold compared with other ceramic bone graft substitutes, supporting faster angiogenesis and bone apposition throughout the defect site, with the development of a functionally adaptive trabecular structure through resorption and remodeling of both scaffold and bone [9]. Due to the desirable properties of osteoinductivity, osteoconductivity, biocompatibility, and biodegradability [10–12], Si-CaP represents a better alternative material for autogenous bone grafting in spinal fusion surgery [10]. Smucker et al. reported that implantation with Si-CaP-30 led to a greater manual palpation and motion analysis fusion rate and superior bone formation than Actifuse ABX and β-Tricalcium Phosphate-Bioactive Glass-Type I Collagen in a rabbit posterolateral spine fusion model [13]. Si-CaP has also been used in the treatment of benign bone defects [14], radius fractures [15], and ankle arthrodesis [16].

However, compared with autogenous bone, a major drawback of Si-CaP is the lack of osteogenic ability [17]. Creating a scaffold that is combined with a substance involved in osteogenic ability may increase the osteogenic potential of the graft substitute material. Studies have shown that autogenous fine particulate bone powder accelerate healing compared with traditional bone grafts [18].

Our team has performed many studies examining AFPBP. We compared AFPBP with autogenous massive bone and found that AFPBP provided sufficient space for cell adhesion and growth. Additionally, more bioactive osteocytes survived than in autogenous massive bone and were involved in the various stages of bone repair. AFPBP also showed direct osteogenetic ability as an ossification center and played a positive role in osteogenesis [19,20]. The rapid resorption of AFPBP could release many bone growth factors, such as BMP-2, TGF-β1, ALP and collagen I, at an early stage of bone repair and reduce osteocytic creeping and substitution [20]. These factors could promote the differentiation of BMSCs into osteoblasts [21]. However, since such particles of the loose bone structure are easily lost, are difficult to mold, and have other shortcomings, the applications are limited.

Therefore, we focused on ways to overcome the respective shortcomings of Si-CaP and AFPBP in spinal fusion. We investigated the potential of viable osteocytes in AFPBP to provide osteogenic properties to the osteoinductivity and osteoconductivity Si-CaP in the combination scaffold: Si-CaP/AFPBP. At present, BMSCs are widely used in bone tissue engineering as seed cells. They can not only differentiate into osteoblasts and exert osteogenic functions but also have advantages of stable growth, rapid proliferation, a high survival rate after inoculation, and easy and less invasive acquisition methods [22]. Thus, in our previous study, we constructed a novel tissue-engineered bone graft composed of Si-CaP, AFPBP, and BMSCs, which exerted good degradation performance, mechanical strength, and biological activity in vitro [21,23]. The scaffold could also induce BMSCs differentiation into osteoblasts and exerted no adverse effects on cell proliferation [23].

Therefore, the purpose of this study was to explore the effects of a novel tissue-engineered bone graft with Si-CaP, AFPBP, and BMSCs in a rabbit posterolateral lumbar fusion model. We verified whether such a combination was effective in promoting spinal fusion and reducing the amount of autogenous bone while achieving bone formation similar to the autogenous bone graft.

Materials and methods

Animals

New Zealand white rabbits of either gender were provided and raised by the animal experiment center of the Second Affiliated Hospital of Harbin Medical University. All animal studies were approved by the Institutional Animal Care and Use Committee of the Second Affiliated Hospital of Harbin Medical University, P.R.China. All animal care and experimental procedures were performed in accordance with the regulations of the Institutional Animal Care and Use Committee of the Second Affiliated Hospital of Harbin Medical University and the “Principles of Laboratory Animal Care” (NIH Publications No. 8023, revised 1978).

Preparation of Si-CaP

We successfully synthesized the Si-CaP by an aqueous precipitation method in our previous study [21]. This composite possessed a silicon content of 0.8 wt%, with a total porosity of 75% and pore size of 150–300 μm.

Preparation of autogenous fine particulate bone powder

After anesthetization of the rabbits with 3% pentobarbital sodium, the 1.2 cm × 0.7 cm × 0.1 cm sections of the ilium weighing 1.25 g were collected from both sides under sterile conditions. Soft tissue such as

connective tissue and cartilage was removed, and the bone was placed in 0.9% physiological saline. It was then ground with a standard bone mill on a fine setting in normal saline until it reached a particulate size of 300–500 μm, and centrifuged to obtain the AFPBP for further use [21].

BMSCs isolation, culture, and identification

BMSCs were isolated and cultured as previously described. Briefly, 4-week-old New Zealand white rabbits after anesthetization were sacrificed by a 20-mL air injection into the marginal ear vein. Bone marrow was harvested from both femurs. BMSCs were isolated from bone marrow by density-gradient centrifugation. The BMSCs were then plated in complete medium consisting of filtered DMEM-F12 and 1% penicillin/streptomycin at 37 °C, 5% CO_2. The medium was refreshed every 3–5 days. Cultured cells from the 3rd passage were counted and prepared for implantation [21]. Morphological identification of BMSCs was performed under a light microscope, and the cell phenotype was verified as described in our previous study [21].

Tracking of CM-Dil-labelled BMSCs

To track the implanted BMSCs, they were stained with CM-Dil. Briefly, BMSCs from the 3rd passage were digested with pancreatin and counted under a microscope. The cell concentration was adjusted to 1×10^7/mL and mixed with CM-Dil (40 μL, 1 g/L) to label 1 mL of the BMSC cell suspension. After incubation at 37 °C for 3 min, the cells were incubated another 15 min on ice. Subsequently, the CM-Dil-labelled BMSCs were added to the Si-CaP/AFPBP grafts.

Preparation of grafts and implantation

Ninety-six animals were divided into four groups: AFPBP, Si-CaP, Si-CaP/AFPBP, Si-CaP/AFPBP/BMSCs. Eight animals in each group were sacrificed by an overdose of pentobarbital sodium at 4, 8, and 12 weeks after implantation, and spinal fusion was evaluated. Si-CaP/AFPBP was prepared by mixing Si-CaP and AFPBP at a 1:1 ratio (0.625 g of each component). BMSCs (1×10^7 cells/mL) at a volume of 0.3 mL were applied to the surface of Si-CaP/AFPBP to construct the Si-CaP/AFPBP/BMSCs graft.

Rabbit posterolateral spinal fusion model

Twelve-week-old skeletally mature New Zealand white rabbits weighing 2.5 kg–3.5 kg of either gender were used to establish a rabbit posterolateral spinal fusion model based on Boden's method [24]. Briefly, the rabbits were anesthetized by intravenous injection of 3% pentobarbital sodium at 1 mL/kg via the ear vein and fixed in the prone position. The spinous processes of L1-L6 are acutely angled in a cephalad direction. In contrast, the L7 spinous process shows much less cranial angulation and is almost perpendicular to the plane of its lamina. A median incision was made from the spinous processes of L4 to L7, creating a greater interspinous distance at L6-L7 compared with the other lumbar levels [25]. From the 5th lumbar to 6th lumbar vertebral plane, the bilateral lumbar dorsal fascia was cut in the lateral 0.5 cm of the mammillary process. Using a high-speed dental grinding drill with a cutting burr, the L5 and L6 transverse processes were decorticated. Then, the grafts were implanted into bilateral sides of the intertransverse process interval, parallel with the spine. All surgeries were performed using aseptic surgical procedures adapted for rabbits. Finally, the implants were covered by the muscle, and the incision was sutured layer by layer and covered with sterile dressing. After the operation, 80,000 U/2 mL of gentamicin was injected subcutaneously to prevent infection once a day for three days. All rabbits were housed in cages in a controlled environment (25 °C and a 12 h light/dark cycle) and fed standard rabbit chow and tap water. Spinal fusion was observed at 4, 8, and 12 weeks after the operation.

Manual palpation of spinal fusion

After administration of anesthesia, the animals were sacrificed and samples of the entire spine were collected by removing the surrounding muscle tissues and ligaments. The segment and adjacent segments were then evaluated for gross motion with gentle flexion extension movements, performed by two blinded investigators. The specimens with an absence of intersegmental motion were rated as fused; they were rated as non-fused if any motion was detected [26].

Radiographic assessment of spinal fusion

After manual palpation, the samples were placed in a microfocal X-ray imaging system (Faxitron X-ray, MX-20, USA) and scanned. The posteroanterior region was viewed and graded by two independent spine surgeons who were blinded to the experiment. According to the modified standard, the fusion degree was divided into 4 grades. Each grade corresponded to a score. The scoring standard was as follows: 0 point, no new bone formation; 1 point, fewer new bone formation; 2 points, moderate and new bone formation and 3 points, a large amount of new bone formation. Grades 2 and 3 were identified as clinical fusion. Unanimous agreement was required to consider a spine completely fused [27].

CT and three-dimensional reconstruction (3D-CT)

The fusion segment was scanned by CT (16 spiral CT, Neuviz, China) and the images were three-dimensionally reconstructed. After scanning, the double-blind method was used to observe and score the spinal fusion condition. The scoring standard was as follows: 0 point, no bone block between bilateral transverse processes; 1 point, bone block in the fusion area on one side; 2 points, no continuous bone block between bilateral transverse processes; 3 points, continuous bone block on one side of the transverse process; 4 points, continuous bone block between bilateral transverse processes. Firm fusion was considered present in specimens with a score of 3 or 4. A score $\leq$2 was considered not fused [28].

Micro-computed tomography

To assess the quality of the newly formed bone between the transverse processes, micro-CT was used. The specimens were scanned and reconstructed with micro-CT (Sedecal, Super Argus, Spain) with the following parameters: 70 kV (voltage), 200 μA (current), 14.8 μm (resolution), 300 ms (exposure time). The following 3-dimensional morphometric parameters were calculated from the developing fusion mass and compared between study groups: bone volume/total volume (BV/TV), trabecular separation (Tb.Sp), trabecular thickness (Tb.Th), connectivity density (Conn.D).

Histology and histomorphometric analysis

The fusion samples were collected and fixed in 4% paraformaldehyde solution, and they were decalcified by immersion in EDTA solution, dehydrated with a graded series of ethanol, soaked serially in xylol, and embedded in paraffin. Longitudinal plane sections (4 μm) from each sample were prepared and stained with hematoxylin and eosin (HE). The samples were then sliced into 4-μm-thick sections along the longitudinal direction of the intertransverse fusion area. After mounting with resinene, the sections were observed at 40×, 100×, and 200× magnification under a microscope.

We randomly selected four histological HE-stained sections at each time point. Images were collected from a field of view magnified at 40× under a microscope. The contour of new bone tissue was outlined. MapInfo software was used to measure the area of new bone formation. The newly formed bone included both woven bone and lamellar bone in the HE-stained images. Then, five horizons were observed for each

section. Differences were compared according to the ratio of new bone formation area to total visual field area.

Scanning electronic microscopy

The samples were cut into 1 cm^3 blocks and fixed with 2% glutaraldehyde for 1 h. The blocks were then fixed with 0.1% osmic acid for 2 h. Next, the specimens were dehydrated with gradient acetone and merged into epoxy resin overnight. Each sample was sectioned into 50–100 nm slices and treated with 1% venturi blue for electron microscopy observation. The interface connection, ultrastructure, and new bone formation between the graft and host bone were examined.

Tracking of CM-Dil-labelled BMSCs and observation

CM-Dil-positive cells in the Si-CaP/AFPBP/BMSCs group were observed by fluorescence microscopy at 4, 8, and 12 weeks after the operation, and were compared with HE-stained sections in the same field of view.

Statistical methods

The data were analyzed using SPSS19.0 statistical software, and the results were expressed as $\overline{X} \pm S$. The results of the manual palpation were compared using the R × C list chi-square test. The X-ray and CT three-dimensional reconstruction data were compared using multiple sets of independent sample rank-sum tests. The micro-CT results were compared using one-way analysis of variance followed by Dunnett's test. $P < 0.05$ was a significant difference.

Results

Animal mortality and complications

Four rabbits in the Si-CaP/AFPBP/BMSCs group died from massive hemorrhage and were replaced with other rabbits. No infection, purulent or other inflammatory reactions were found in the operation area in any group. All rabbits were able to walk on the first postoperative day.

Manual palpation

No fusion had occurred in any group at 4 weeks after surgery; therefore, no comparison was made. At 8 weeks, analysis using manual palpation revealed that the fusion rate in the Si-CaP/AFPBP/BMSCs group (87.5%) was higher than in the AFPBP (75%) ($P > 0.05$), Si-CaP/AFPBP (62.5%) ($P > 0.05$) and Si-CaP groups (12.5%) ($P < 0.05$). At 12 weeks, the manual palpation fusion rates in the Si-CaP/AFPBP/BMSCs and AFPBP groups both reached 100%, which was higher than the Si-CaP/AFPBP group (62.5%) ($P > 0.05$). However, fusion was obtained in only 3/8 samples (37.5%) in the Si-CaP group ($P < 0.05$) (Fig. 1).

Radiographic analysis of spinal fusion

No firm fusions were observed in any group at 4 weeks. By radiographs, evidence of bone formation on the decorticated host bone transverse processes was observed at 8 weeks in all groups. Over time, the new bone formed and remodeled, leading to fusions at 12 weeks in each group (Fig. 2A). Similarly, the radiographic scores increased in all groups from weeks 4–12, indicating a time-dependent osteogenetic process. The scores of the AFPBP, Si-CaP/AFPBP, and Si-CaP/AFPBP/BMSCs groups were higher than the Si-CaP group. At each time point, the scores of the Si-CaP/AFPBP/BMSCs group were equivalent to the AFPBP group and significantly higher than the Si-CaP group ($P < 0.05$) (Table 1).

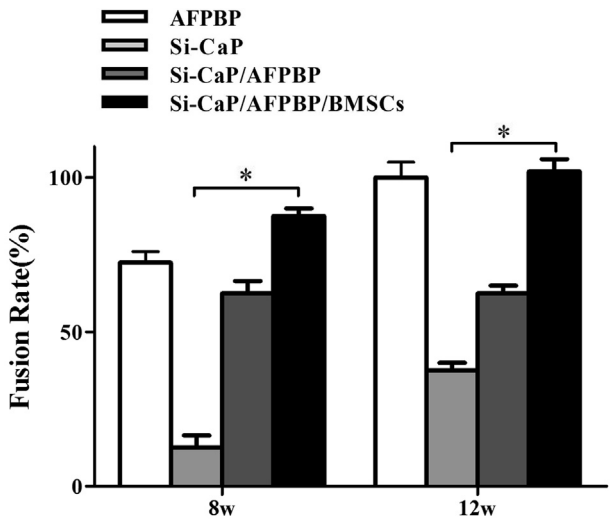

Fig. 1. The fusion rate results by manual palpation in each group at 8 and 12 weeks after the operation. AFPBP, autogenous fine particulate bone powder; BMSCs, bone marrow mesenchymal stem cells; Si-CaP, silicon-substituted calcium phosphate. Data were expressed as the mean ± SEM. n = 8. *P < 0.05.

3D-CT evaluation of spinal fusion

At 4, 8, and 12 weeks after surgery, the CT scores in the Si-CaP/AFPBP/BMSCs group tended to be higher than those in the Si-CaP/AFPBP and AFPBP groups, but this result did not achieve statistical significance ($P > 0.05$). The CT scores in the Si-CaP/AFPBP/BMSCs group were significantly higher than in the Si-CaP group ($P < 0.05$) (Table 2). At 12 weeks, the 3D-CT images further showed obvious bone connections between bilateral transverse processes, and the fusion area between bilateral transverse processes was stable. The bone mass continuously fused the transverse processes, and the fusion mass was larger in the Si-CaP/AFPBP/BMSCs group (Fig. 2B).

Micro-CT analysis of spinal fusion

The BV/TV, Tb.Th, Conn.D, and Tb.Sp values at 4, 8, and 12 weeks after the operation in each group were evaluated by micro-CT examination. The BV/TV, Tb.Th, and Conn.D values in the Si-CaP/AFPBP/BMSCs group were significantly higher than those in the Si-CaP/AFPBP and Si-CaP groups ($P < 0.05$) (Fig. 3A–C). The Tb.Sp values in the Si-CaP/AFPBP/BMSCs group were significantly lower than those in the Si-CaP/AFPBP and Si-CaP groups ($P < 0.05$) (Fig. 3D). However, the data were comparable to those in the AFPBP group. The micro-CT images were shown in Fig. 2C. Bone formation in the Si-CaP/AFPBP/BMSCs group was similar to the AFPBP group.

Histological examination and histomorphometric analysis

In the AFPBP group, a large amount of woven bone formed, many osteoblasts were observed around the woven bone, and osteocytes were observed in the bone lacunae at 4 weeks. The majority of the bone grafts had been replaced by newly formed woven bone and cartilage, and osteoblasts were observed on the surface of the woven bone. Blood vessels and marrow cavities were observed at 8 weeks. At 12 weeks, woven bone had been replaced by lamellar bone. The marrow cavities were unobstructed (Fig. 4 A13).

In the Si-CaP group, a large amount of fibrous tissue was observed, the Si-CaP was partially degraded, and there was no obvious formation of bone at 4 weeks. The Si-CaP had been slowly absorbed, and a small amount of woven bone and few osteoblasts were observed at 8 weeks. Si-CaP was further degraded. A small amount of woven bone had formed,

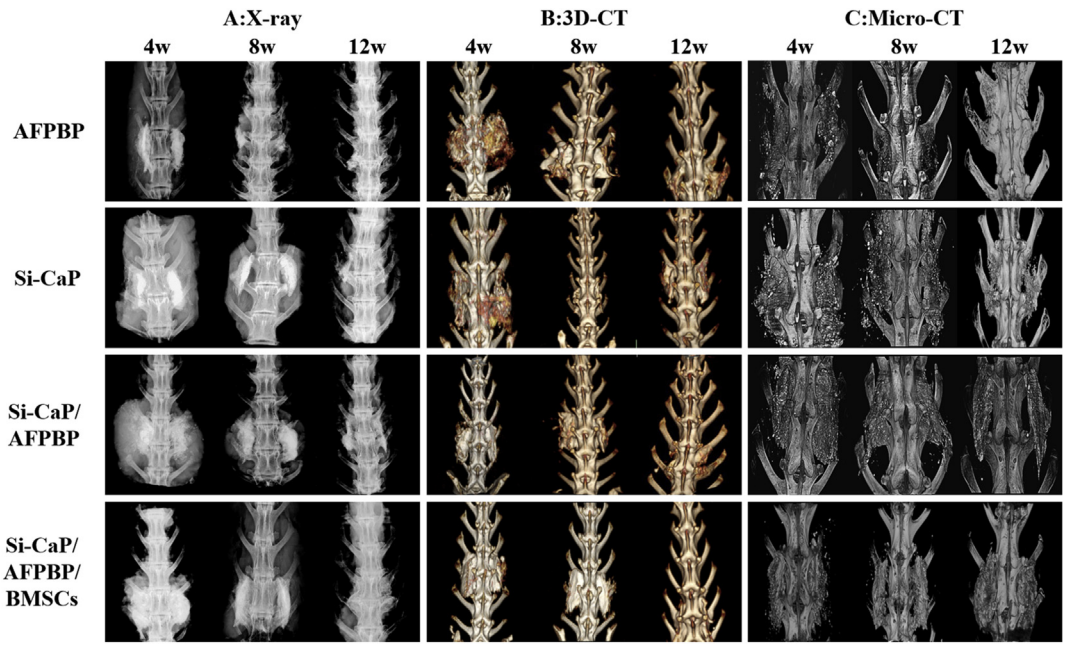

Fig. 2. Spinal fusion evaluated by X-ray (A), 3D-CT (B) and micro-CT (C). AFPBP, autogenous fine particulate bone powder; BMSCs, bone marrow mesenchymal stem cells; Si-CaP, silicon-substituted calcium phosphate.

Table 1
Bone fusion scores determined by X-ray analysis.

	X-ray scores				Average rank	χ^2	*P*
	0	1	2	3			
4-week data							
AFPBP	0	6	2	0	30.25	27.773	0.000
Si-CaP	7	1	0	0	11.75*		
Si-CaP/AFPBP	3	5	0	0	20.75		
Si-CaP/AFPBP/BMSCs	0	6	2	0	30.25		
8-week data							
AFPBP	0	2	0	6	29.00	26.367	0.000
Si-CaP	5	2	1	0	12.75*		
Si-CaP/AFPBP	3	0	2	3	21.00		
Si-CaP/AFPBP/BMSCs	0	0	1	7	31.25		
12-week data							
AFPBP	0	0	0	8	31.50	32.252	0.000
Si-CaP	4	1	2	1	13.88*		
Si-CaP/AFPBP	0	3	4	1	19.13		
Si-CaP/AFPBP/BMSCs	0	0	0	8	31.50		

*P < 0.05 vs Si-CaP/AFPBP/BMSCs.

Table 2
Bone fusion scores determined by three-dimensional CT reconstruction.

	3D-CT Scores					Average rank	χ^2	*P*
	0	1	2	3	4			
4-week data								
AFPBP	0	0	6	2	0	30.25	27.268	0.000
Si-CaP	6	1	1	0	0	12.44*		
Si-CaP/AFPBP	3	0	5	0	0	29.56		
Si-CaP/AFPBP/ BMSCs	0	0	6	2	0	30.25		
8-week data								
AFPBP	0	0	0	2	6	30.75	28.439	0.000
Si-CaP	5	1	0	2	0	13.06*		
Si-CaP/AFPBP	3	0	0	4	1	18.63		
Si-CaP/AFPBP/ BMSCs	0	0	1	0	7	31.56		
12-week data								
AFPBP	0	0	0	0	8	30.00	34.052	0.000
Si-CaP	1	4	0	3	0	13.13*		
Si-CaP/AFPBP	0	0	3	0	5	24.38		
Si-CaP/AFPBP/ BMSCs	0	0	0	0	8	30.00		

*P < 0.05 vs Si-CaP/AFPBP/BMSCs.

and osteoblasts were observed around the woven bone at 12 weeks (Fig. 4 B13).

In the Si-CaP/AFPBP group, along with the absorption of Si-CaP and AFPBP, small amounts of woven bone were recognized and some osteoblasts were observed around the graft material at 4 weeks. At 8 weeks, the Si-CaP gradually decreased. New bone formation continued and increased obviously compared with the 4-week assessment, and osteoblasts were observed. A small amount of Si-CaP was unabsorbed, and trabecular could be seen between transverse processes at 12 weeks. Abundant lamellar bone and osteoblasts were observed, and a few marrow cavities were unobstructed (Fig. 4 C13).

In the Si-CaP/AFPBP/BMSCs group, Si-CaP and AFBFP were partially absorbed, a small amount of woven bone was recognized, and some osteoblasts were observed around the graft material at 4 weeks. At 8 weeks, the degradation of Si-CaP was evident and new woven bone had markedly increased compared with that at 4 weeks. We also observed bone formation via endochondral ossification. At 12 weeks, Si-CaP were almost completely degraded, and a large area of woven bone was replaced by lamellar bone. The marrow cavities and blood vessels were completely unobstructed (Fig. 4 D13).

Histomorphometry data, represented in Fig. 5, were consistent with the general histological observation of the fusion mass. In all groups, the proportion of bone in the fusion mass steadily increased over time, showing a significant trend. At 4 weeks, a higher proportion of bone was determined in the AFPBP group (23.49%) compared with the Si-CaP/AFPBP/BMSCs group (14.66%, P < 0.05). In the Si-CaP/AFPBP/BMSCs group at 8 weeks, the area percentage of new bone formation was 28.56%, which was less than in the AFPBP group (33.21%, P < 0.05). However, no difference in bone volume was observed between the Si-CaP/AFPBP/BMSCs (44.39%) and AFPBP group (45.06%) at 12 weeks (P > 0.05).

Scanning electronic microscopy (SEM) examination

At 12 weeks, new trabecular were visible in each group. In the Si-

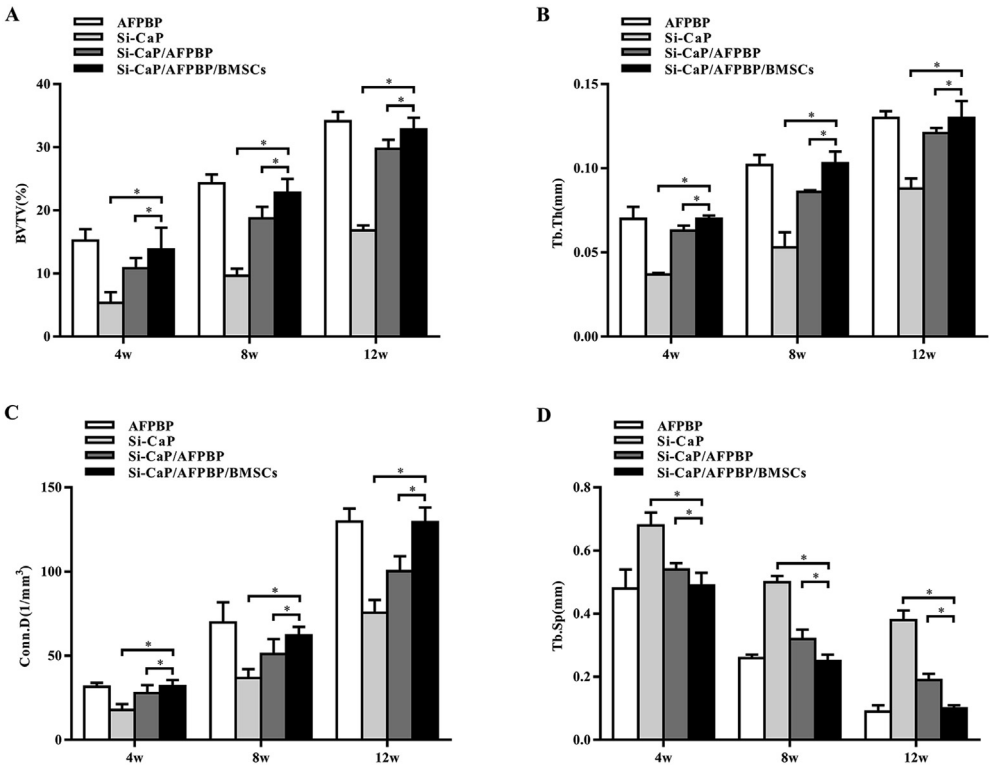

Fig. 3. The BV/TV, Tb.Th, Conn.D, and Tb.Sp values at 4, 8, and 12 weeks after the operation in each group were evaluated by micro-CT. BV/TV, bone volume/total volume; Tb.Sp, trabecular separation; Tb.Th, trabecular thickness; Conn.D, connectivity density. AFPBP, autogenous fine particulate bone powder; BMSCs, bone marrow mesenchymal stem cells; Si-CaP, silicon-substituted calcium phosphate. Data were expressed as the mean ± SEM. n = 8. *P < 0.05.

CaP/AFPBP/BMSCs and AFPBP groups, a large number of new trabecular were formed. The trabecular were arranged irregularly, forming a large amount of new bone and numerous irregular marrow cavities. The scattered Si-CaP adhered to the surface of the trabecular in the Si-CaP/AFPBP/BMSCs group (Fig. 6 A. D). There were fewer new trabecular in the Si-CaP/AFPBP group than the above two groups. The trabecular were irregularly arranged, and a small amount of undegraded Si-CaP could be seen on the surface (Fig. 6 C). New trabecular could barely be found in the Si-CaP group. The Si-CaP were partially degraded and absorbed. Simultaneously, the trabecular were arranged irregularly and passed through the pores that formed after the absorption of Si-CaP (Fig. 6 B).

Tracking of CM-Dil-labelled BMSCs and observation in grafts

The red fluorescent signal of CM-Dil-positive cells in the spinal fusion zones were visualized using fluorescence microscopy after Si-CaP/AFPBP/BMSCs group implantation at 4, 8, and 12 weeks, which confirmed the presence of the implanted BMSCs. When the images were investigated, CM-Dil-positive cells were observed in the soft tissue and bone matrix at 4 weeks after implantation (Fig. 7A and B); throughout 8 weeks of implantation, the CM-Dil-positive osteocytes and chondrocytes were observed in the cartilage and bone matrices (Fig. 7C and D); and at 12 weeks after implantation, CM-Dil-positive osteocytes were distributed in the new bone lacunae (Fig. 7E).

Discussion

Spinal fusion is used for the treatment of multiple spinal conditions, including trauma, infection, tumor, and malformation [1]. The bone graft placed between the transverse processes has been shown to play a key role in posterolateral lumbar fusion. The autogenous bone graft is still the gold standard for posterolateral lumbar fusion because of its properties of osteoconduction, osteoinduction, and osteogenesis [2]. Nevertheless, the nonunion rate with the use of an autogenous bone grafts in patients can be as high as 25%–36% [29]. Moreover, limited bone graft sources and donor site morbidity have hindered their extensive use, especially in cases in which large amounts of bone graft material are required. The development of bone tissue engineering as an alternative approach for spinal fusion has opened up new fields for the study of ideal autogenous bone substitute materials [30].

The concept of bone tissue engineering shows that the scaffold serves as a template for cell interactions and the formation of bone extracellular matrix [7]. It also provides a structural support for the newly formed bone [30]. Typically, four types of biomaterials are used to fabricate such scaffolds: ceramics, polymers, metals, and composites [8]. Calcium phosphate (CaP) is a popular ceramics material as a kind of scaffold due to its biocompatible and bioresorbable characteristics. It is also similar to the inorganic bone structure of the human body with porous features, which improves osteoconductive ability [8]. However, because of its poor absorption, brittleness, and biodegradability, CaP will slowly affect new bone formation and late development to some extent [8]. Silicon is often utilized as a substituent or a dopant in bioceramics, since it enhances the ultimate properties of conventional biomaterials such as the surface chemical structure, mechanical strength, bioactivity, and biocompatibility [31]. Gibson et al. showed that the silicon ion radius is similar to the phosphorus ion radius [32]. Therefore, when adding a certain concentration of silicon, calcium-containing calcium phosphate materials not only can promote osteoblast proliferation, but also exhibit high osteoclast-mediated bioabsorbability [33]. However, compared with autogenous bone, a major drawback of Si-CaP is the lack of osteogenic ability [17]. In our previous study, we confirmed that AFPBP contained more living osteocytes, created blood vessel growth faster, released more growth factors, absorbed faster, and had a higher bone formation rate than autogenous massive bone [19,20]. To improve the osteogenic properties of the Si-CaP and reduce the amount of autogenous bone, we combined AFPBP with Si-CaP. The addition of BMSCs or

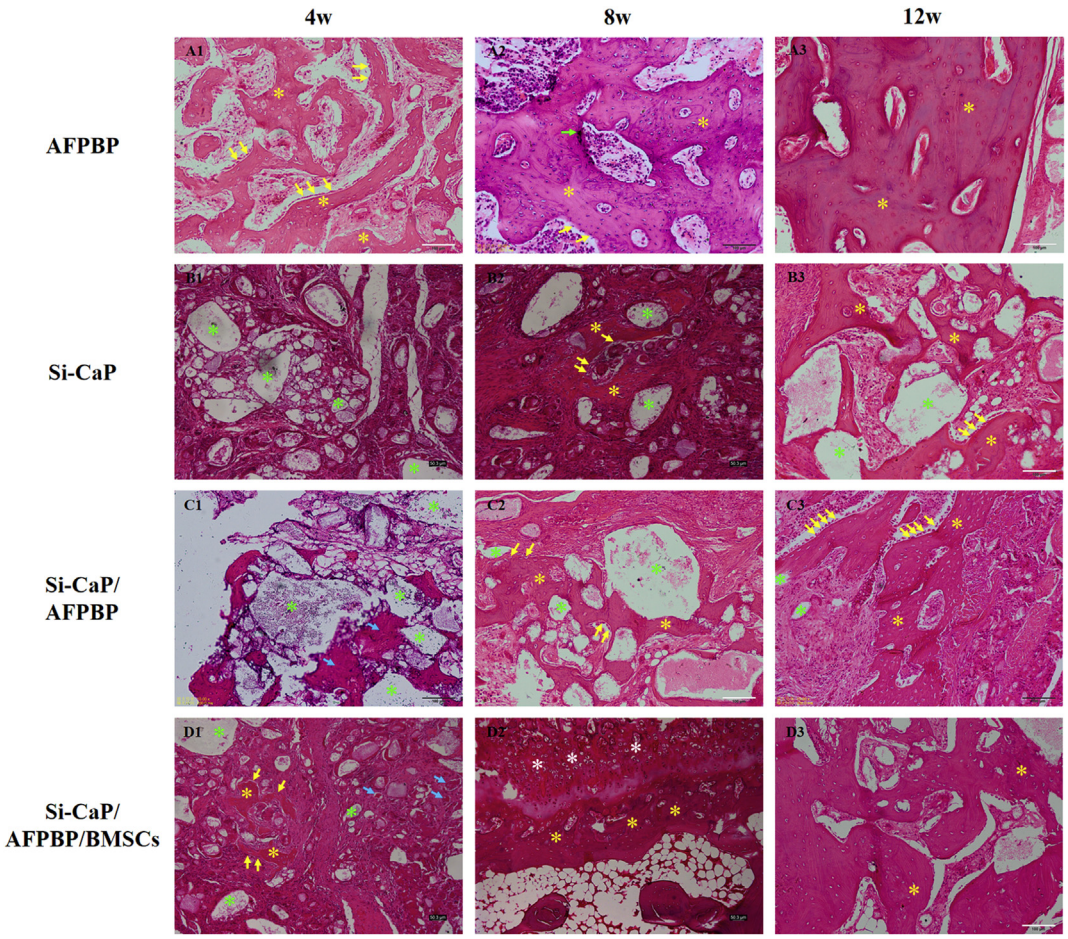

Fig. 4. Histological sections in each group at 4, 8, and 12 weeks after the operation (yellow arrows: osteoblasts, yellow asterisks: newly formed bone, green arrows: osteoclasts, green asterisks: Si-CaP, blue arrows: AFBFP, white asterisks: chondrocytes).

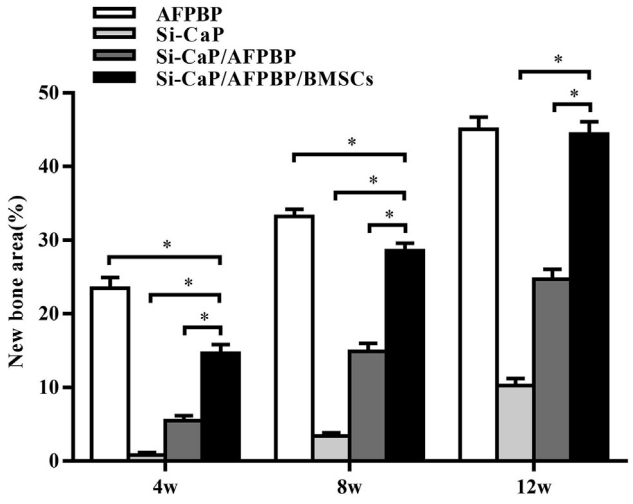

Fig. 5. Statistical analysis of histological sections of new bone area in each group at 4, 8, and 12 weeks after the operation. AFPBP, autogenous fine particulate bone powder; BMSCs, bone marrow mesenchymal stem cells; Si-CaP, silicon-substituted calcium phosphate. Data were expressed as the mean ± SEM. n = 20 sections from 3 animals. *P < 0.05.

osteogenic-inducing factors to scaffolds has been reported as a potential strategy to improve the biological performance of biomaterials [22]. In our previous study, we constructed a novel tissue-engineered bone graft composed of Si-CaP, AFPBP, and BMSCs. We found that it exerted good degradation performance, mechanical strength, and biological activity in vitro [21,23]. The scaffold could also induce BMSCs differentiation into osteoblasts and exerted no adverse effects on cell proliferation [23].

Hence, the composite consisting of Si-CaP/AFPBP with BMSCs was introduced to promote spinal fusion for the first time in this study. The well-reported model developed by Boden was used in this study [34]. This animal model overcomes the limitations of previous models by more closely replicating the human procedure in relation to the surgical technique, graft healing environment, and outcomes [34]. The nature of this posterolateral model provides insights into the osteoconductive response of a material as well as a more generalized osteogenic response, when you consider the material–host interactions adjacent to a bony bed (osteoconductive response) and in the middle of the transverse process (osteogenic response) [35].

In this study, we confirmed that Si-CaP/AFPBP together with BMSCs could achieve spinal fusion. The manual palpation results showed that the fusion rate was higher in the Si-CaP/AFPBP/BMSCs group than the AFPBP, Si-CaP/AFPBP and Si-CaP groups at 8 weeks. This finding suggested that bone formation occurred earlier in the Si-CaP/AFPBP/BMSCs group than the AFPBP group. At 12 weeks, the fusion rate in the AFPBP group reached 100%, compared with 62.5% in the Si-CaP/AFPBP group. The addition of BMSCs to the Si-CaP/AFPBP composite increased the fusion rate from 62.5% to 100%, which was the same as the AFPBP group. There was no significant difference between the fusion rates of the Si-CaP/AFPBP/BMSCs and AFPBP groups by manual palpation at 8 weeks and 12 weeks, suggesting that Si-CaP/AFPBP/BMSCs in the spinal fusion was comparable to AFPBP. While manual palpation could distinguish a non-fused segment, it represented a subjective assessment of the

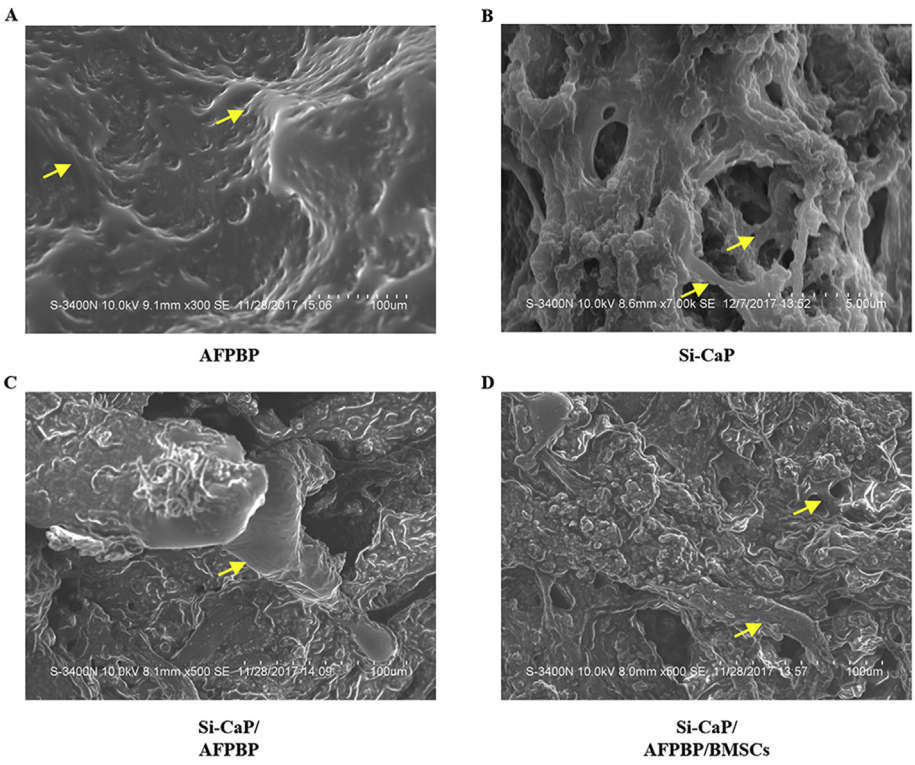

Fig. 6. Bone formation was evaluated by scanning electron microscopy (SEM) examination at 12 weeks after the operation. Yellow arrows: trabecular

stiffness rather than the strength of the fusion.

Therefore, we chose the radiology assessment by X-ray and 3D-CT technology because it could provide relatively clear images for examining fusion. Application of the corresponding scoring system was also helpful for quantitative analyses of imaging findings. At all three time points, the scores of the Si-CaP/AFPBP/BMSCs group were equivalent to that of the AFPBP group and significantly higher than that of the Si-CaP group. In the radiographic evaluation, no solid fusion was observed at 4 weeks after surgery. Subsequently, bone formation on the transverse processes was observed at 8 weeks in all groups. The new bone formed and remodeled, leading to fusions at 12 weeks in each group. These results were also confirmed by the 3D-CT observations at 4 weeks and 8 weeks. However, the bone connections were obvious between bilateral transverse processes, and the fusion area between bilateral transverse processes was stable at 12 weeks. The bone mass continuously fused the transverse processes, and the fusion mass was larger in the Si-CaP/AFPBP/BMSCs group. However, due to resolution constraints and subjective factors, it was impossible to accurately describe the fusion at each time point solely by radiology methods, especially at the time of early integration of trabecular during the beginning of formation.

Micro-CT has a higher resolution and can determine the trabecular index more accurately and objectively [36]. Thus, the X-ray and 3D-CT scores in the Si-CaP/AFPBP/BMSCs group were only significantly higher than in the Si-CaP group, but the data by micro-CT analysis were significantly different in the Si-CaP/AFPBP/BMSCs group from both the Si-CaP/AFPBP group and the Si-CaP group. The micro-CT data at 4, 8, and 12 weeks after the operation showed that the bone volume fraction, trabecular thickness and trabecular junction density gradually increased while the trabecular space gradually decreased in the Si-CaP/AFPBP/BMSCs, Si-CaP/AFPBP, and AFPBP groups. These findings were consistent with the regular pattern of new bone formation.

Studies have shown that Si-CaP possesses a strong surface protein adsorption capacity and has the ability to promote the attachment of human mesenchymal stem cells and osteoblasts and the differentiation of MSCs into osteoblasts [37]. Our histological observations revealed that the effect of Si-CaP was consistent with the above findings. Compared with the Si-CaP group, the Si-CaP/AFPBP/BMSCs group began to absorb at an early stage, and a large number of osteoblasts, osteoclasts, chondrocytes, and new bone matrix could be observed. Histologically, we observed Si-CaP remaining inside new bone in the Si-CaP group at all 3 time points (Fig. 4 B13) and in the Si-CaP/AFPBP group at 4 (Fig. 4 C1) and 8 weeks (Fig. 4 C2). These results indicated that the degradation rate of Si-CaP was lower than that of bone formation in the specific osseous soft tissue environment of the posterior spine. It is also noteworthy that a number of Si-CaP granules were encapsulated in soft tissue and separated from the nascent bone tissues (Fig. 4 B3; C3). Although, new trabecular were visible in each group at 12 weeks, the Si-CaP were still partially degraded and absorbed based on the SEM observations. These results were consistent with the histological findings. The above phenomenon above should be associated with the study of Lerner et al. They combined Si-CaP with bone marrow extract as a bone graft material during posterior scoliosis correction. New bone growth was observed at 3 and 5 months. At 9 months after surgery, the trabecular bone graft material was observed in the vertebral body [38]. Thus, compared with 9 months, longer time points beyond 12 weeks were not examined in our study. It is necessary to further verify the conclusions of our study in a large animal model in future research. However, the degradation rate of Si-CaP/AFPBP/BMSCs matched the rate of bone formation, with almost no Si-CaP granules inside the new bone.

The histomorphometric analysis showed that the area percentage of new bone formation was higher in the AFPBP group than the Si-CaP/AFPBP/BMSCs group at 4, 8, and 12 weeks after surgery. However, there was no significant difference between the two groups at 12 weeks. Histological examination also showed large numbers of osteoblasts, chondrocytes, and osteocytes in the Si-CaP/AFPBP/BMSCs group. Whether these cells we found were differentiated from the BMSCs we applied to the scaffold or not? CM-Dil is a type of lipophilic carbocyanine dye that strongly bonds to the cellular phospholipid layer with excellent light stability, a long labeling time, and no cytotoxicity [39]. Therefore, we used CM-Dil to mark BMSCs and observed them by fluorescence microscopy. Qi et al. used the CM-Dil-labelled BMSCs in their study and found that by detecting CM-Dil positive cells, red fluorescence was

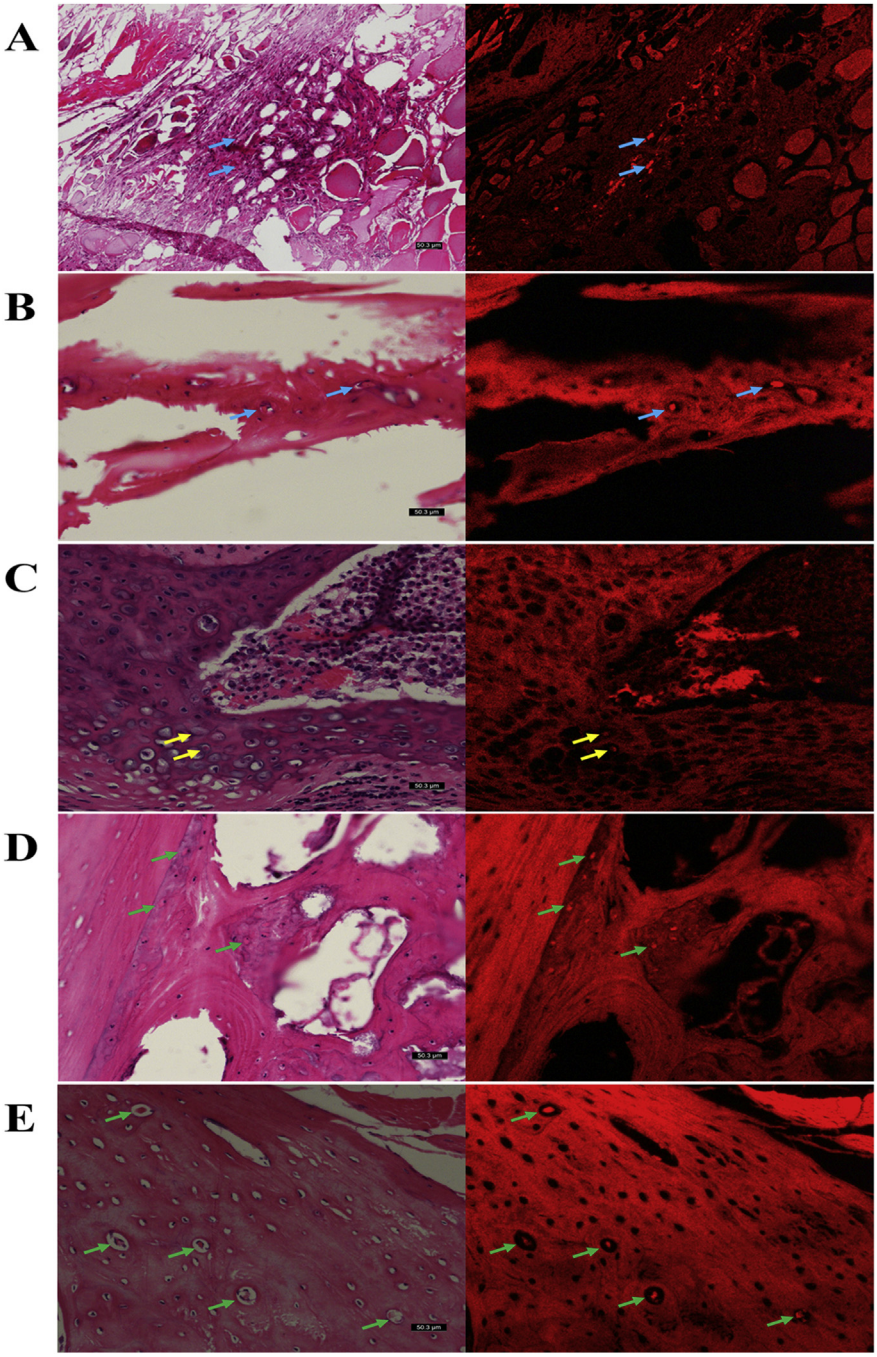

Fig. 7. CM-Dil-positive cells in the Si-CaP/AFPBP/BMSCs group were observed by fluorescence microscopy at 4, 8, and 12 weeks after the operation compared with HE-stained sections in the same field of view. (A) CM-Dil-positive cells (blue arrows) in soft tissue at 4 weeks; (B) CM-Dil-positive cells (blue arrows) in bone matrix at 4 weeks; (C) CM-Dil-expressing chondrocytes (yellow arrows) in cartilage matrix at 8 weeks; (D) CM-Dil-positive osteocytes (green arrows) in bone matrix at 8weeks; (E) CM-Dil-positive osteocytes (green arrows) in the new bone lacunae at 12 weeks.

emitted in the bone defect area and a large number of CM-Dil positive cells could be observed in new bone [40]. We also visualized the red fluorescent signal of CM-Dil-positive cells in the spinal fusion zones after Si-CaP/AFPBP/BMSCs group implantation at 4, 8, and 12 weeks confirming the presence of the implanted BMSCs. When compared with HE-stained sections in the same field of view, we found that the BMSCs participated in various stages of osteogenesis by differentiating into osteoblasts, chondrocytes, and osteocytes.

In the Si-CaP/AFPBP group, we unexpectedly found that the spinal fusion could be also promoted. Si-CaP and AFPBP were mixed at a mass ratio of 1:1, and the amount of bone used was only half of that in the AFPBP group, which reduced the amount of autogenous bone for spinal fusion. However, the osteogenic effect was worse in the Si-CaP/AFPBP group than the Si-CaP/AFPBP/BMSCs and AFPBP groups. Similarly, the radiographic images of the X-ray and 3D-CT reconstruction also revealed a larger bone formation area in the Si-CaP/AFPBP/BMSCs group than the Si-CaP/AFPBP group. Newly formed bone was more obvious and appeared earlier in the Si-CaP/AFPBP/BMSCs group than the Si-CaP/AFPBP group.

Fredericks et al. compared the effects of Si-CaP, autogenous bone, and Si-CaP/autogenous bone (volume ratio 1:3) on spinal fusion at 12 weeks after operation in a posterolateral spinal fusion rabbit model [41]. They found that the effects of Si-CaP or Si-CaP/autogenous bone were similar to the effects of autogenous bone, indicating that Si-CaP can be used as a substitute for the autogenous bone graft [41]. In our study, the fusion rate that occurred in the Si-CaP/AFPBP composite (mass ratio was 1:1) was higher than that reported in Fredericks' study. Compared with that study, we achieved more extensive fusion and used less autogenous bone, because AFPBP shows better bone formation ability than autogenous massive bone [18–20].

The present study supported the excellent bioactivity of Si-CaP/AFPBP/BMSCs. The characteristics of this novel tissue-engineered bone graft were related to the nature of the components. First, silicon contributed to the development of the mineralized skeleton and upregulation of osteoblastic cells. The role of Si enhanced the biological performance of the CaP, for instance, the differentiation and proliferation of osteoblasts, bone apposition, and in-growth. Second, Si-CaP provided a trabecular structure similar to that of cancellous bone. The struts were macroporous and microporous with high levels of interconnectivity, accelerating osseointegration. Additionally, the Si-CaP combination with other grafts provided a graft with a negative surface charge to yield a positive effect on osteoblast activity and neovascularization of the bone. It also provided a more stable osteoconductive scaffold compared with other ceramic bone graft substitutes, supporting faster angiogenesis and bone apposition with the development of a functionally adaptive trabecular structure through resorption and remodeling of both the scaffold and bone. Moreover, the addition of AFPBP endowed Si-CaP with osteogenic properties, because AFPBP has a large surface area that might allow it to release more growth factors. The enlarged surface area enhanced the ability of cells to absorb nutrients and encouraged cell survival. The porosity of AFPBP supported the growth of tiny blood vessels. Hence, the Si-CaP/AFPBP scaffold promoted BMSCs attachment, proliferation, and osteoblastic differentiation in the absence of osteogenic factors. The fusion efficacy of Si-CaP/AFPBP/BMSCs was superior to that of Si-CaP/AFPBP and Si-CaP, but equivalent to that of AFPBP. This novel tissue-engineered bone graft showed similar osteoinductivity, osteoconductivity, biocompatibility, and biodegradability to autogenous bone. It reduced the required amount of autogenous bone and promoted spinal fusion in rabbits.

We recognize the limitations of this study. First, biomechanical testing was not examined. Second, the limited sample numbers may have an impact on the reliability of the test results. Further studies are needed to compare the abilities of BMSCs/Si-CaP, BMSCs/AFPBP, and BMSCs in promoting spinal fusion. These issues can be resolved in future investigations.

Conclusion

This study demonstrated for the first time that Si-CaP/AFPBP/BMSCs is a novel tissue-engineered bone graft with excellent bioactivity, biocompatibility, and biodegradability. The graft could reduce the amount of autogenous bone and promote spinal fusion in a rabbit posterolateral lumbar fusion model, representing a novel alternative to autogenous bone with great potential clinical applications.

Funding information

This study was supported by the National Natural Science Foundation of China (Grant numbers: 81371977 and 81772362).

Conflict of Interest

The authors have no conflicts of interest to disclose in relation to this article.

Acknowledgements

The authors would like to thank the technical help from the Key Laboratory of Myocardial Ischemia of Harbin Medical University, Ministry of Education, Heilongjiang Province, China.

References

[1] Qu Y, Wang B, Chu B, Liu C, Rong X, Chen H, et al. Injectable and thermosensitive hydrogel and PDLLA electrospun nanofiber membrane composites for guided spinal fusion. ACS Appl Mater Interfaces 2018;10(5):4462–70. https://doi.org/10.1021/acsami.7b17020.

[2] Kroeze RJ, Smit TH, Vergroesen PP, Bank RA, Stoop R, van Rietbergen B, et al. Spinal fusion using adipose stem cells seeded on a radiolucent cage filler: a feasibility study of a single surgical procedure in goats. Eur Spine J 2015;24:1031–42. https://doi.org/10.1007/s00586-014-3696-x.

[3] Kawecki F, Clafshenkel WP, Fortin M, Auger FA, Fradette J. Biomimetic tissue-engineered bone substitutes for maxillofacial and craniofacial repair: the potential of cell sheet technologies. Adv Healthc Mater 2018;7(6):e1700919. https://doi.org/10.1002/adhm.201700919.

[4] Saifi C, Bernhard J, Shillingford JN, Petridis P, Robinson S, Guo XE, et al. Tissue engineered bone differentiated from human adipose derived stem cells inhibit posterolateral fusion in an athymic rat model. Spine 2018;43(8):533–41. https://doi.org/10.1097/BRS.0000000000002384.

[5] Shin DA, Yang BM, Tae G, Kim YH, Kim HS, Kim HI. Enhanced spinal fusion using a biodegradable porous mesh container in a rat posterolateral spinal fusion model. Spine J 2014;14:408–15. https://doi.org/10.1016/j.spinee.2013.08.038.

[6] Page JM, Prieto EM, Dumas JE, Zienkiewicz KJ, Wenke JC, Brown-Baer P, et al. Biocompatibility and chemical reaction kinetics of injectable, settable polyurethane/allograft bone biocomposites. Acta Biomater 2012;8(12):4405–16. https://doi.org/10.1016/j.actbio.2012.07.037.

[7] Vergroesen PP, Kroeze RJ, Helder MN. The use of poly(L-lactide-co-caprolactone) as a scaffold for adipose stem cells in bone tissue engineering: application in a spinal fusion model. Macromol Biosci 2011;11(6):722–30. https://doi.org/10.1002/mabi.201000433.

[8] Hammouche S, Hammouche D, McNicholas M. Biodegradable bone regeneration synthetic scaffolds: in tissue engineering. Curr Stem Cell Res Ther 2012;7(2):134–42. https://doi.org/10.2174/157488812799219018.

[9] Hing KA, Wilson LF, Buckland T. Comparative performance of three ceramic bone graft substitutes. Spine J 2007;7:475–90. https://doi.org/10.1016/j.spinee.2006.07.017.

[10] Gillespie P, Wu G, Sayer M, Stott MJ. Si complexes in calcium phosphate biomaterials. J Mater Sci Mater Med 2010;21(1):99–108. https://doi.org/10.1007/s10856-009-3852-8.

[11] Xu W, Ganz C, Weber U, Adam Holzhüter G, Wolter D, Frerich B, et al. Evaluation of injectable silica-embedded nanohydroxyapatite bone substitutein a rat tibia defect model. Int J Nanomed 2011;6:1543–52. https://doi.org/10.2147/IJN.S19743.

[12] Coathup MJ, Samizadeh S, Fang YS, Buckland T, Hing KA, Blunn GW. The osteoinductivity of silicate-substituted calcium phosphate. J Bone Joint Surg Am 2011;93(23):2219–26. https://doi.org/10.2106/JBJS.I.01623.

[13] Smucker JD, Petersen EB, Al-Hili A, Nepola JV, Fredericks DC. Assessment of SiCaP-30 in a rabbit posterolateral fusion model with concurrent chemotherapy. Iowa Orthop J 2015;35:140–6. https://doi.org/10.1109/ICNSC.2008.4525364.

[14] Kirschner HJ, Obermayr F, Schaefer J. Treatment of benign bone defects in children with silicate-substituted calcium phosphate (SiCaP). Eur J Pediatr Surg 2012;22(2):143–7. https://doi.org/10.1055/s-0032-1308699.

[15] Leroux T, Perez-Ordonez B, von Schroeder HP. Osteolysis after the use of a silicon-stabilized tricalcium phosphate-based bone substitute in a radius fracture: a case report. J Hand Surg Am 2007;32(4):497–500. https://doi.org/10.1016/j.jhsa.2007.01.005.

[16] Pomeroy GC, DeBen S. Ankle arthrodesis with silicate-substituted calcium phosphate bone graft. Foot Ankle Online J 2013;6(1):2. https://doi.org/10.3827/faoj.2013.0601.002.

[17] Hutchens SA, Campion C, Assad M, Chagnon M, Hing KA. Efficacy of silicate-substituted calcium phosphate with enhanced strut porosity as a standalone bone graft substitute and autograft extender in an ovine distal femoral critical defect model. J Mater Sci Mater Med 2016;27(1):20. https://doi.org/10.1007/s10856-015-5559-3.

[18] Chuang JP, Chang CP, Shen HT, Kao J, Yan JL. Repair of the canine vertebral lamina with a combination of autologous micromorselized bone and poly-lactic acid gel after a total laminectomy. Kaohsiung J Med Sci 2010;26:357–65. https://doi.org/10.1016/S1607-551X(10)70059-0.

[19] Wang XT, Zhou CL, Yan JL, Yan X, Xie HX, Sun CL. The fate of donor osteocytes in fine particulate bone powders during repair of bone defects in experimental rats. Acta Histochem 2012;114(3):192–8. https://doi.org/10.1016/j.acthis.2011.04.010.

[20] Sun YX, Sun CL, Tian Y, Xu WX, Zhou CL, Xi CY, et al. A comparison of osteocyte bioactivity in fine particulate bone powder grafts vs larger bone grafts in a rat bone repair model. Acta Histochem 2014;116(6):1015–21. https://doi.org/10.1016/j.acthis.2014.04.004.

[21] Tian Y, Cui LH, Xiang SY, Xu WX, Chen DC, Fu R, et al. Osteoblast-oriented differentiation of BMSCs by co-culturing with composite scaffolds constructed using silicon-substituted calcium phosphate, autogenous fine particulate bone powder and alginate in vitro. Oncotarget 2017;8(51):88308–19. https://doi.org/10.18632/oncotarget.19015.

[22] Huang J, Wang Daming, Chen Jielin, Liu Wei, Duan Li, You Wei, et al. Osteogenic differentiation of bone marrow mesenchymal stem cells by magnetic nanoparticle composite scaffolds under a pulsed electromagnetic field. Saudi Pharmaceut J 2017;25:575–9. https://doi.org/10.1016/j.jsps.2017.04.026.

[23] Sun C, Tian Y, Xu W, Zhou C, Xie H, Wang X. Development and performance analysis of Si-CaP/fine particulate bone powder combined grafts for bone regeneration. Biomed Eng Online 2015;14:47. https://doi.org/10.1186/s12938-015-0042-4.

[24] Virk SS, Coble D, Bertone AL, Hussein HH, Khan SN. Experimental design and surgical approach to create a spinal fusion model in a New Zealand white rabbit

(Oryctolagus cuniculus). J Invest Surg 2017;30(4):226–34. https://doi.org/10.1080/08941939.2016.1235748.
[25] Palumbo M, Valdes M, Robertson A, Sheikh S, Lucas P. Posterolateral intertransverse lumbar arthrodesis in the New Zealand White rabbit model: I Surgical anatomy. Spine J 2004;4(3):287–92. https://doi.org/10.1016/S1529-9430(03)00565-5.
[26] Hu MH, Lee PY, Chen WC, Hu JJ. Comparison of three calcium phosphate bone graft substitutes from biomechanical, histological, and crystallographic perspectives using a rat posterolateral lumbar fusion model. Mater Sci Eng C Mater Biol Appl 2014;45:82–8. https://doi.org/10.1016/j.msec.
[27] Curylo LJ, Johnstone B, Petersilge CA, Janicki JA, Yoo JU. Augmentation of spinal arthrodesis with autologous bone marrow in a rabbit posterolateral spine fusion model. Spine 1999;24(5):434–8. https://doi.org/10.1097/00007632-199903010-00004.
[28] Klineberg E, Haudenschild DR, Snow KD, Garitty S, Christiansen BA, Acharya C, et al. The effect of noggin interference in a rabbit posterolateral spinal fusion model. Eur Spine J 2014;23(11):2385–92. https://doi.org/10.1007/s00586-014-3252-8.
[29] Noshchenko A, Hoffecker L, Lindley EM, Burger EL, Cain CM, Patel VV. Perioperative and long-term clinical outcomes for bone morphogenetic protein versus iliac crest bone graft for lumbar fusion in degenerative disk disease: systematic review with meta-analysis. J Spinal Disord Tech 2014;27(3):117–35. https://doi.org/10.1097/01.bsd.0000446752.34233.ca.
[30] Wang H, Zhou Y, Li CQ, Chu TW, Wang J, Huang B. Tissue-engineered bone used in a rabbit model of lumbar intertransverse process fusion: a comparison of osteogenic capacity between two different stem cells. Exp Therapeut Med 2020;19(4):2570–8. https://doi.org/10.3892/etm.2020.8523.
[31] Khan AF, Saleem M, Afzal A, Ali A, Khan A, Khan AR. Bioactive behavior of silicon substituted calcium phosphate based bioceramics for bone regeneration. Mater Sci Eng C Mater Biol Appl 2014;35:245-252. https://doi.org/10.1016/j.msec.2013.11.013.
[32] Gibson IR, Best SM, Bonfield W. Chemical characterization of silicon-substituted hydroxyapatite. J Biomed Mater Res 1999;44(4):422–8. https://doi.org/10.1002/(sici)1097-4636(19990315)44:4<422::aid-jbm8>3.0.co;2-#.
[33] Lehmann G, Cacciotti I, Palmero P, Montanaro L, Bianco A, Campagnolo L, et al. Differentiation of osteoblast and osteoclast precursors on pure and silicon-substituted synthesized hydroxyapatites. Biomed Mater 2012;7(5):055001. https://doi.org/10.1088/1748-6041/7/5/055001.
[34] Boden SD, Schimandle JH, Hutton WC. An experimental lumbar intertransverse process spinal fusion model Radiographic, histologic, and biomechanical healing characteristics. Spine 1995;20(4):412–20. https://doi.org/10.1097/00007632-199502001-00003.
[35] Walsh WR, Vizesi F, Cornwall GB, Bell D, Oliver R, Yu Y. Posterolateral spinal fusion in a rabbit model using a collagen-mineral composite bone graft substitute. Eur Spine J 2009;18(11):1610-1620. https://doi.org/10.1007/s00586-009-1034-5.
[36] Feldkamp LA, Goldstein SA, Parfitt AM, Jesion G, Kleerekoper M. The direct examination of three-dimensional bone architecture in vitro by computed tomography. J Bone Miner Res 1989;4(1):3–11. https://doi.org/10.1002/jbmr.5650040103.
[37] Cameron K, Travers P, Chander C, Buckland T, Campion C, Noble B. Directed osteogenic differentiation of human mesenchymal stem/precursor cells on silicate substituted calcium phosphate. J Biomed Mater Res A 2013;101(1):13–22. https://doi.org/10.1002/jbm.a.34261.
[38] Lerner T, Liljenqvist U. Silicate-substituted calcium phosphate as a bone graft substitute in surgery for adolescent idiopathic scoliosis. Eur Spine J 2013;22(Suppl 2):S185-S194. https://doi.org/10.1007/s00586-012-2485-7.
[39] Darkazalli A, Levenson CW. Tracking stem cell migration and survival in brain injury: current approaches and future prospects. Histol Histopathol 2012;27(10):1255–61. https://doi.org/10.14670/HH-27.1255.
[40] Qi Y, Niu L, Zhao T, Shi Z, Di T, Feng G, et al. Combining mesenchymal stem cell sheets with platelet-rich plasma gel/calcium phosphate particles: a novel strategy to promote bone regeneration. Stem Cell Res Ther 2015;6:256. https://doi.org/10.1186/s13287-015-0256-1.
[41] Fredericks DC, Petersen EB, Sahai N, Corley KG, DeVries N, Grosland NM, et al. Evaluation of a novel silicate substituted hydroxyapatite bone graft substitute in a rabbit posterolateral fusion model. Iowa Orthop J 2013;33:25–32.